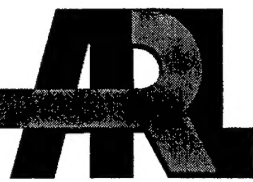


ARMY RESEARCH LABORATORY



Galvanic Behavior Database for Titanium-Steel Alloy Couples

by Ralph P. I. Adler, Christopher E. Miller, and Brian E. Placzankis

ARL-TR-2812

September 2002

Approved for public release; distribution is unlimited.

20020926 064

NOTICES

Disclaimers

The findings in this report are not to be construed as an official Department of the Army position unless so designated by other authorized documents.

Citation of manufacturer's or trade names does not constitute an official endorsement or approval of the use thereof.

Destroy this report when it is no longer needed. Do not return it to the originator.

Army Research Laboratory

Aberdeen Proving Ground, MD 21005-5069

ARL-TR-2812

September 2002

Galvanic Behavior Database for Titanium-Steel Alloy Couples

Ralph P. I. Adler, Christopher E. Miller, and Brian E. Placzankis
Weapons and Materials Research Directorate, ARL

Abstract

Future lightweight armor for the next generation of lighter material will probably use titanium alloy components. These will form galvanic couples with other materials and may induce phenomena accelerating the corrosion rate of those metals less noble than titanium. The project objective was to evaluate the magnitude of galvanic corrosion between typical ferrous and titanium alloys. Electrochemical and accelerated corrosion measurements on both bare and Chemical agent resistant coatings (CARC)-coated Ti/steel samples determined accelerated corrosion rates. Samples with and without "X-scribed" defects in the CARC coating were evaluated. Electrochemical studies on bare Ti/steel couples validated accelerated steel corrosion rates but found that intact CARC coatings mitigate corrosion. Even for X-scribed samples, the rapid corrosion product buildup in the defect reduced galvanic currents by two orders of magnitude. Studies with "Joint A Assembly" CARC-coated samples (phase I: bolted sets of Ti/steel plates with intact CARC seals) had virtually no interface corrosion. After examination, the rebolted samples with compromised CARC seals had a second accelerated corrosion cycle (phase II); the moisture intrusion caused a severe buildup of interface corrosion. Thus Ti/Fe interfaces with defect-free CARC coatings can prevent buildup of iron corrosion products.

Acknowledgments

The authors want to recognize the following colleagues for their contributions to this report: Russell A. Kilbane who was responsible for the setup and experimental measurement of potentiodynamic scans and galvanic corrosion cell testing for galvanic corrosion. Dr. Paul F. Buckley for his initiation of and technical contributions to this project. Dr. Daniel J. Snoha for his expertise in operating the x-ray diffraction equipment and providing quality powder diffraction results. Finally, Dr. John H. Beatty for his technical leadership and professional advice.

INTENTIONALLY LEFT BLANK.

Contents

Acknowledgments	iii
List of Figures	vii
List of Tables	ix
1. Introduction	1
2. Experimental Procedure	1
2.1 Experimental Test Plan	1
2.1.1 Scientific Assessment of Galvanic Corrosion.....	1
2.1.2 Engineering Assessment of Galvanic Corrosion.....	1
2.2 Sample Preparation.....	2
2.2.1 Scientific Test Samples	2
2.2.2 Engineering Test Samples.....	2
2.3 Testing Protocol	4
2.3.1 Testing Protocol for Scientific Samples.....	4
2.3.2 Testing Protocol for Engineering Samples.....	5
3. Results and Discussion	6
3.1 Scientific Evaluations.....	6
3.2 Engineering Evaluations.....	9
3.2.1 Salt Fog Exposure Results.....	9
3.2.2 Cyclic Corrosion Exposure Results.....	9
3.2.3 X-ray Characterization of Interface Corrosion Products From Post-Phase II (CCT and SFT) “TACOM Joint A Assembly” Samples.....	10
4. Conclusions	12
4.1 Scientific Studies.....	12
4.2 Engineering Studies.....	15
5. References	17
Report Documentation Page	19

INTENTIONALLY LEFT BLANK.

List of Figures

Figure 1. Engineering samples assembled to the “TACOM Joint A Assembly” configuration.....	3
Figure 2. Electrochemical cell assembly for scientific testing.	4
Figure 3. ASTM B117 SFT chamber.....	5
Figure 4. GM9540 P cyclic test chamber.....	6
Figure 5. Potentiodynamic scans for Ti (upper trace in blue) and Fe (trace in red).	7
Figure 6. Corrosion products on AISI 4130 after 14 days galvanic cell test, (a) no. 4 exposed to 0.5N NaCl and (b) no. 2 exposed to 0.005N NaCl.	8
Figure 7. Macrophotos of Ti-steel interfaces after phase I salt fog exposure.....	11
Figure 8. Macrophotos of Ti-steel interfaces after phase II salt fog exposure.	11
Figure 9. Assembled armor mockup couples after phase II GM 9540P testing exposure.....	12
Figure 10. Macrophotos of Ti-steel interfaces after phase I cyclic corrosion exposure.....	13
Figure 11. Macrophotos of Ti-steel interfaces after phase II cyclic corrosion exposure.....	13
Figure 12. Macrophotos of Fe-Fe interfaces after phase II salt fog exposure.	14
Figure 13. Macrophotos of Fe-Fe interfaces after phase II cyclic corrosion exposure.....	14

INTENTIONALLY LEFT BLANK.

List of Tables

Table 1. Potentiodynamic testing.....	1
Table 2. Galvanic corrosion cell testing (Ti 6/4 against 4130).....	2
Table 3. Assessment of galvanic current parameters for Ti/Fe couple.....	8
Table 4. X-ray diffraction data for iron oxide phase analysis.....	9
Table 5. Interpretation of corrosion products from galvanic cell Fe substrates.....	9
Table 6. “Joint A Assembly” interface corrosion rating system.....	10
Table 7. “Joint A Assembly” interface corrosion assessment after salt fog exposure.....	10
Table 8. “Joint A Assembly” interface corrosion assessment after cyclic corrosion exposure....	12
Table 9. Interface oxidation products for “Joint A Assembly” samples from x-ray diffraction analysis.....	15

INTENTIONALLY LEFT BLANK.

1. Introduction

Future lightweight armor materials will be required for the next generation of “lighter and more lethal and more survivable” materiel. This will involve the use of state-of-the-art, low-cost titanium alloy components [1] that will most likely be in electrical contact with structural and armor steels as well as other materials. The resulting galvanic couples thus may induce galvanic corrosion phenomena and could dramatically accelerate the corrosion rate of the metal that is usually less noble than the titanium alloy. The specific objective of this project was to evaluate the magnitude of galvanic corrosion effects between typical ferrous and titanium alloys. Electrochemical and accelerated corrosion measurements were taken from both bare and chemical agent resistant coatings (CARC)-coated Ti/steel samples to determine the galvanically accelerated corrosion rates and whether these reach unacceptable rates when a liquid electrolyte is present. This gives an indication of the maximum galvanically assisted corrosion rates expected because U.S. Army vehicles are often covered with (a film of) water. Comparison between bare couples and those with CARC coatings (with and without “defects”) in an aqueous environment will indicate the magnitude of the phenomenon and whether further corrosion prevention/inhibition remedies are necessary. For CARC-coated Ti/steel couples there must be a demonstration that the 15-year corrosion resistance performance is met with a CARC system that also meets the Environmental Protection Agency’s compliance goals for FY05.

2. Experimental Procedure

2.1 Experimental Test Plan

2.1.1 Scientific Assessment of Galvanic Corrosion

See Tables 1 and 2.

Table 1. Potentiodynamic testing.

Alloy	Concentration of NaCl in Cell Electrolyte
Ti 6/4	3.5%
AISI 4130	3.5%

2.1.2 Engineering Assessment of Galvanic Corrosion

Accelerated corrosion testing using “Salt Fog Testing” per American Society for Testing of Materials (ASTM) Standard B117 [2] and cyclic corrosion testing per the GM 9540P

Table 2. Galvanic corrosion cell testing (Ti 6/4 against 4130).

Condition	Concentration of NaCl in Cell Electrolyte
Bare couple	0.005N
Bare couple	0.5N
CARC coating (w/o defects)	0.005N
CARC coating (w/o defects)	0.5N
CARC coating (w/scratch defect)	0.005N
CARC coating (w/scratch defect)	0.5N

protocol [3] was performed on CARC-coated “TACOM* Joint A Assembly” samples [4]. Specific combinations (Ti/Ti; Ti/Fe; and Fe/Fe) of Ti 6/4 and 4130 plates were through-hole bolted together with a grade 8 fastener followed by thorough CARC coating. Both phase I accelerated corrosion testing protocols involved testing each assembly with an intact interface sealed by the CARC coating. After phase I, each couple was disassembled and the internal common plate interface examined. The re-assembled sample with its broken CARC-interface seal, which then allows fluid entrainment, was then resubjected to a second series (phase II) with an identical sequence of phase I accelerated testing exposures.

2.2 Sample Preparation

2.2.1 Scientific Test Samples

Samples for electrochemical and engineering testing were produced from existing supplies of Titanium 6/4 (6 w/o aluminum; 4 w/o vanadium) alloy and American Iron and Steel Institute (AISI) 4130 steel. All scientific test samples had two parallel faces, but size and shape varied. Prior to potentiodynamic or galvanic corrosion cell testing, the “bare” specimens were abraded with 600-grit silicon carbide paper, rinsed in distilled water, degreased in acetone, rinsed again in distilled water, and then dried. One square centimeter of each bare specimen was exposed to the test solution. The “coated” samples had the machined surfaces pretreated with DOD-P-15328 [5], then primed with MIL-P-53022 [6], and topcoated with MIL-C-53039 [7]. One square centimeter of each “coated” specimen with or without an “X-scribed” defect was exposed to the test solution.

2.2.2 Engineering Test Samples

Engineering samples were assembled to the “TACOM Joint A Assembly” configuration that is described schematically in Figure 1. $2 \times 2 \times 1$ -in plates of Ti and steel were individually grit-blasted to a near-white finish. Then specific combinations (Ti/Ti; Ti/Fe; and Fe/Fe) of these plates were “through-hole bolted together” with a grade 8 fastener torqued to 180 ft-lb. Each assembly, including the bolt/nut and washer, was then pretreated with DOD-P-15328 [5], then liberally primed with MIL-P-53022 [6], and then topcoated with MIL-C-53039 [7] that formed an effective seal against fluid intrusion.

* TACOM = U.S. Army Tank-automotive and Armaments Command.

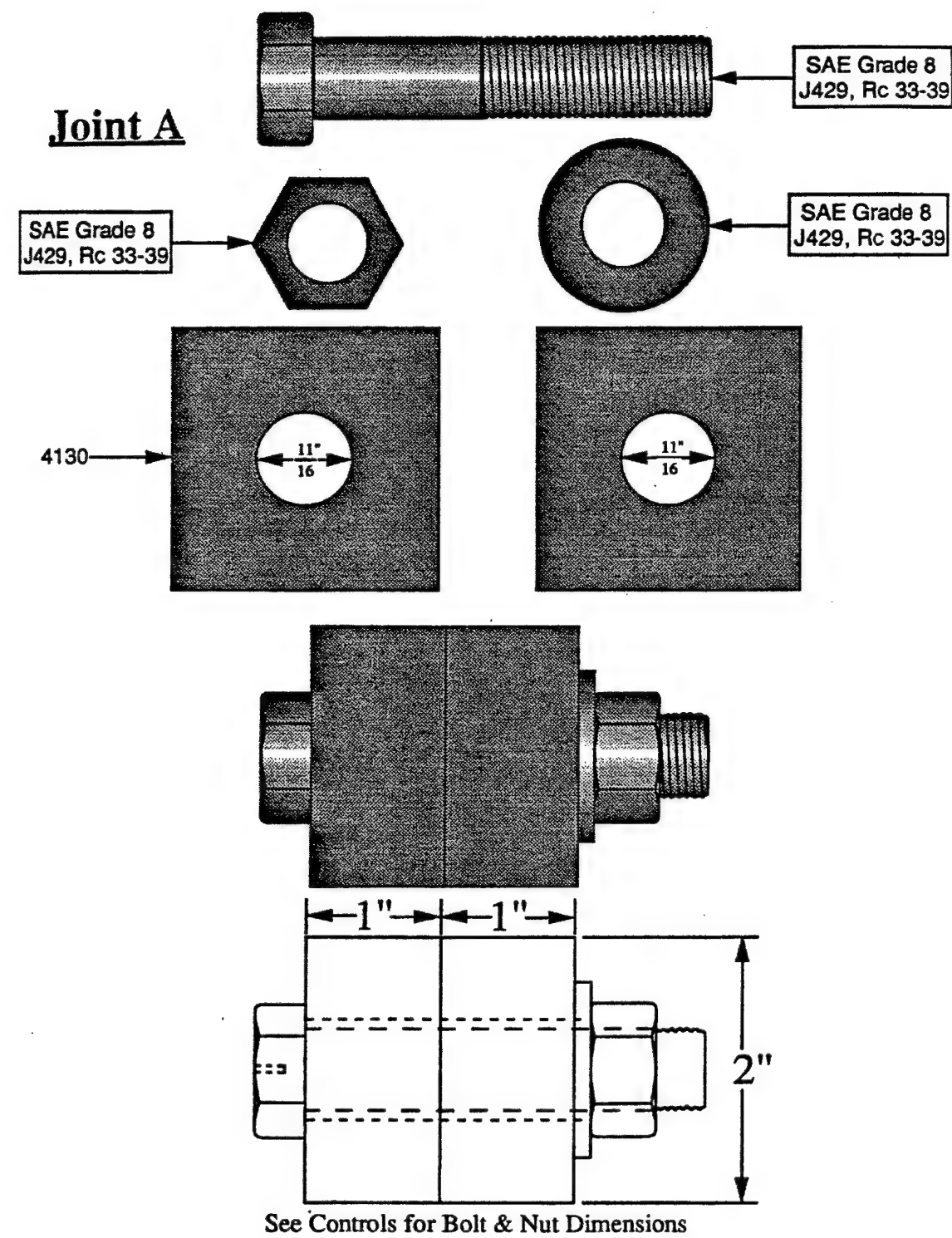


Figure 1. Engineering samples assembled to the "TACOM Joint A Assembly" configuration.

2.3 Testing Protocol

2.3.1 Testing Protocol for Scientific Samples

More specific details and a description of the equipment used can be found in Miller et al. [8]. Figure 2 depicts the electrochemical cell assembly that was used for both series of scientific tests.

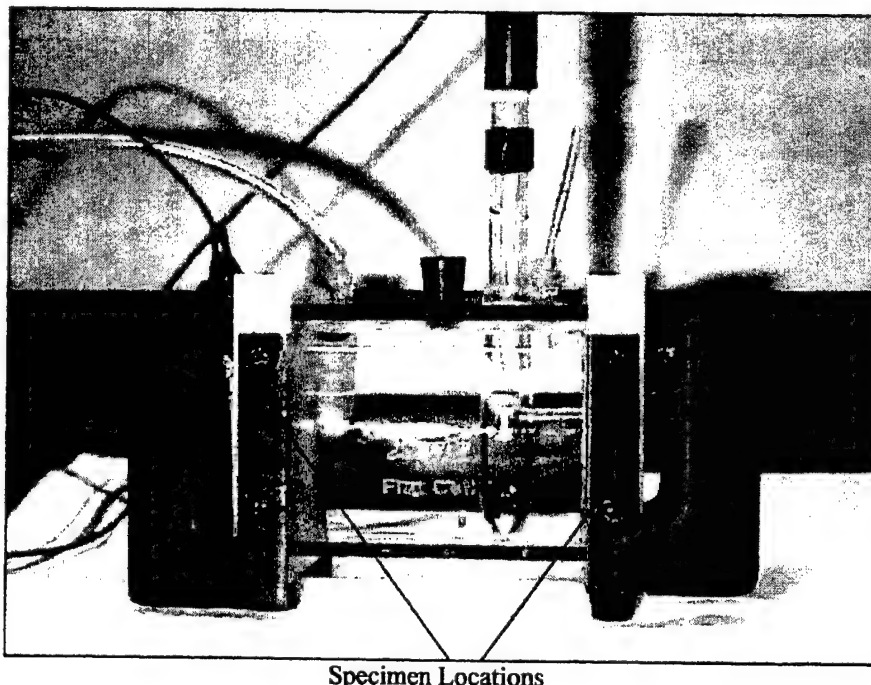


Figure 2. Electrochemical cell assembly for scientific testing.

Potentiodynamic tests were conducted at room temperature in an aerated cell containing about 400 mL of the test solution. The model K0235 cells were manufactured by Princeton Applied Research (PAR), with a platinum-plated electrode at one end of the cell and a sample holder at the other end. A computer-controlled Schlumberger SI 1280 electrochemical measurement unit was used. The open-circuit potentials were measured against a saturated calomel electrode (SCE) for one hour before the scans commenced. A scan rate of 0.1667 mV/s was used. Potentiodynamic scans were performed in standard 3.5% NaCl aqueous solutions.

Galvanic tests were performed in two concentrations of salt solutions (0.5N and 0.005N NaCl), but could not be performed in distilled water due to its high resistivity. For high humidity atmospheric exposures, the 0.5N NaCl solution may be too severe but was still run for comparative reasons. A modified version of the PAR K0235 with sample holders at both ends for coupling the Ti 6/4 and 4130 specimens was used for the galvanic corrosion tests (Figure 2). In this test setup, a Keithley* Multiplexer with single-pole double-throw switches was used to

* Keithley is a trademark of Test Instrumentation Group, 28775 Aurora Road, Cleveland, OH 44139.

sequentially multiplex between each of the six (nitrogen) aerated cells and a PAR 273 Potentiostat/Galvanostat. A potential difference between samples of 0 V was maintained (an effective short circuit) while simultaneously measuring the galvanic current (I) that is proportional to the corrosion rate. The galvanic currents were measured over a minimum of two weeks (for the bare and defect-free coated samples) or four weeks for the coated samples with X-scribed defects (to reach an apparent steady state current value).

2.3.2 Testing Protocol for Engineering Samples

2.3.2.1 Salt Fog Testing (SFT). SFT of “TACOM Joint A Assembly” samples were performed according to ASTM B117 [2] protocol in two phases. Figure 3 shows the SFT chamber and lists the exposure parameters. The phase I exposure of 2500 hr was performed with an unbroken CARC seal. After unbolting and breaking the CARC seal, the interface was examined for any corrosion phenomena. Subsequently each couple, after one plate was rotated by 90° and rebolted to snug fit state, was given a second 2500-hr exposure (phase II) without the benefit of the original CARC seal. Sample interface characterization was then again documented.

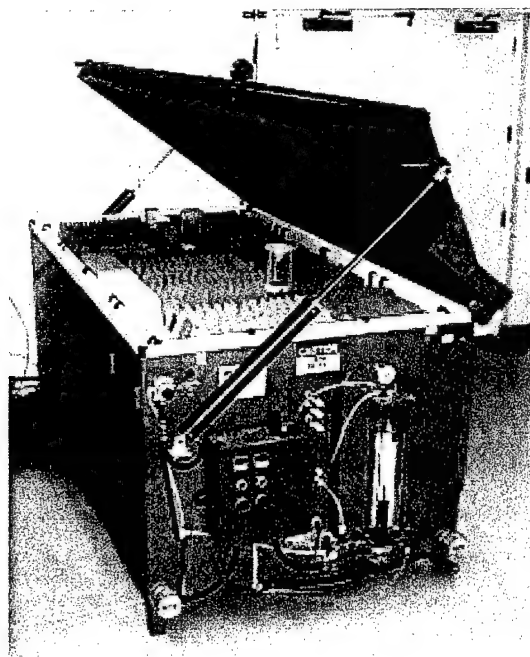


Figure 3. ASTM B117 SFT chamber.

ASTM B117-90 Test Chamber

- 95 F @ 100% RH
- 5% (by weight) NaCl Solution
- Compressed Air Atomized Fog

2.3.2.2 Cyclic Corrosion Testing (CCT). CCT of another series of “TACOM Joint A Assembly” samples were performed according to General Motors (GM) 9540P [3] protocol in two phases. Figure 4 shows the cyclic test chamber and lists the exposure parameters. The phase I exposure of 100 cycles was performed with an unbroken CARC seal. After unbolting and breaking the CARC seal, the interface was examined for any corrosion phenomena.

GM 9540P Cyclic Test Chamber

- 0.9% NaCl
- 0.25 NaHCO₃
- 0.1% CaCl₂

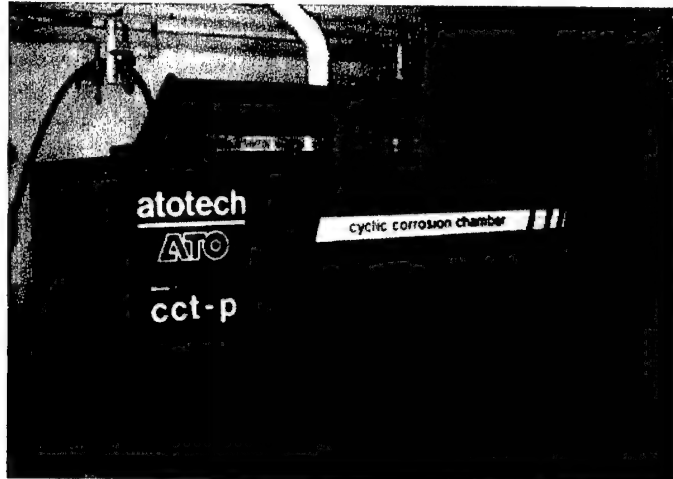


Figure 4. GM9540 P cyclic test chamber.

Subsequently each couple, after one plate was rotated by 90° and rebolted to snug fit state, was given a second 100-cycle exposure (phase II) without the benefit of the original CARC seal. Sample interface characterization was then again documented.

3. Results and Discussion

3.1 Scientific Evaluations

The potentiodynamic scans for the Ti and steel samples in 3.5% NaCl aqueous solution are shown in Figure 5. The various electrochemical parameters were estimated as follows: (1) corrosion potential for Ti 6/4 = -0.35 V, (2) corrosion potential for AISI 4130 = -0.8V, and (3) mixed corrosion potential (for Ti 6/4 with AISI 4130) = -0.75 V. Note that the mixed corrosion current was an order of magnitude greater than that for the corrosion current for AISI 4130.

Galvanic current is a useful indicator of the behavior of two different materials that are in electrical contact with each other in a specific environment. Larger currents indicate that galvanically assisted corrosion is occurring that is proportional to the effective contact area and the galvanic potential difference between the materials in the coupled sample. Smaller currents

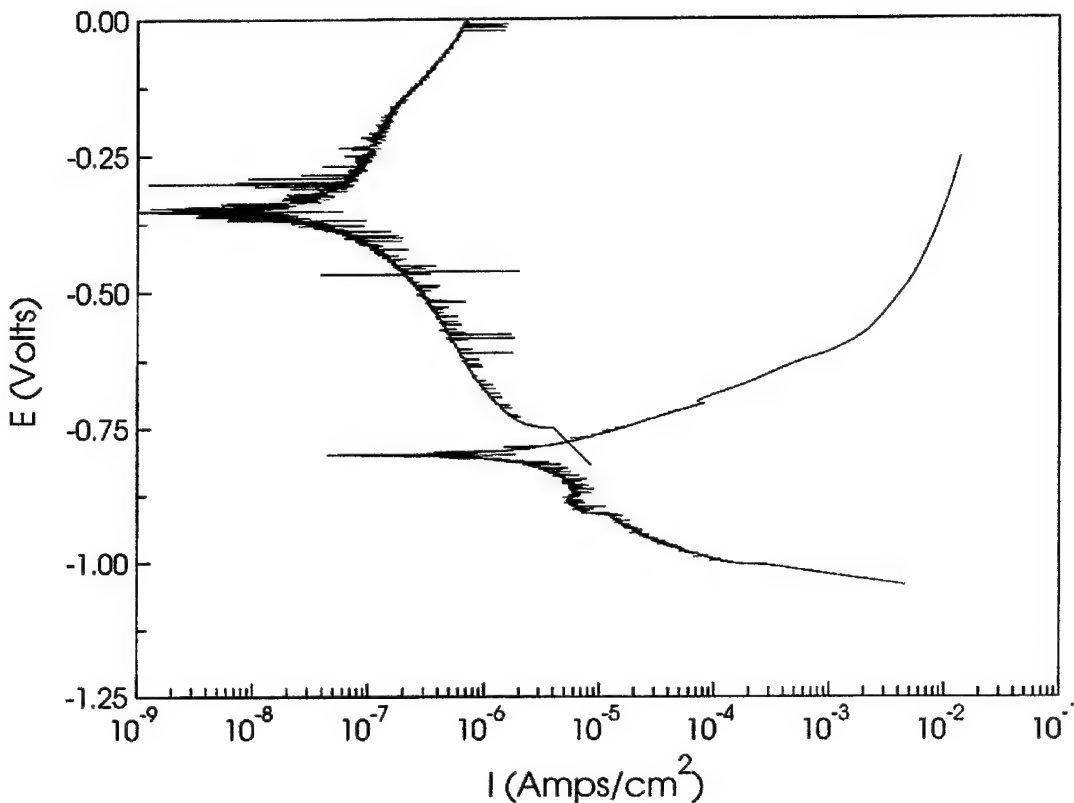


Figure 5. Potentiodynamic scans for Ti (upper trace in blue) and Fe (trace in red).

indicate that either there is a small galvanic differential between the materials or that the kinetics of the corrosion reaction are quite slow. If the current decreases with exposure time, it may be that the buildup of corrosion products acts as a partial barrier. In the present case, the galvanic current (I) provides an assessment of the relative corrosion rates as a function of electrolytic salt concentration for bare and CARC-coated samples as well as CARC-coated samples with deliberately X-scribed defects. The results and observations are listed in Table 3.

Characterization of the corrosion products on the bare iron substrates is depicted in Figure 6 for samples exposed to 0.005N and 0.5N NaCl solutions (sample nos. 4 and 2, respectively) and has also been included in the next series of tables.

X-ray results were obtained using a “2 theta” flat sample diffractometer with Cu K-alpha radiation [9]. By measuring and then ratioing the intensities of the strongest diffraction peaks from the iron substrate and the two iron oxide phases (i.e., magnetite $[Fe_3O_4]$ and hematite $[Fe_2O_3]$), information about the corrosion products formed on the 4130 steel substrate during the “bare” galvanic current tests can be obtained. The relevant x-ray diffraction data is listed in Table 4. Analysis of this x-ray diffraction data has been interpreted to show that the concentration of NaCl in the electrolyte produces differences in total oxide thickness and the relative volume fraction of the hematite and magnetite phases and is presented in Table 5.

Table 3. Assessment of galvanic current parameters for Ti/Fe couple.

Parameters		Max. Current		Steady State Current		Comments
Solute Conc 0.005 N NaCl	Sample	Magnitude (μ A/sq. cm.)	Nominal Time (Days)	Magnitude (μ A/sq. cm.)	Nominal Time (Days)	
0.005	Bare Couple	20	2	10	6-14	similar behavior for bare couples whether in 0.5 or 0.005 solns.
	CARC-coated with X-scribed Defect	0.18	5	0.12	20	very small steady state Galvanic current
	CARC-coated, Defect Free	zero		zero		CARC very protective, no Galvanic current
0.5	Bare Couple	18	2	6-8	4-10	rapid build-up of thicker corrosion product reduces current relative to 0.005N exposures
	CARC-coated with X-scribed Defect	Approaches steady state		0.006	7-14	rapid buildup of corrosion product in defect significantly reduces Galvanic current relative to 0.005N exposure
	CARC-coated, Defect Free	zero		zero		CARC very protective, no Galvanic current

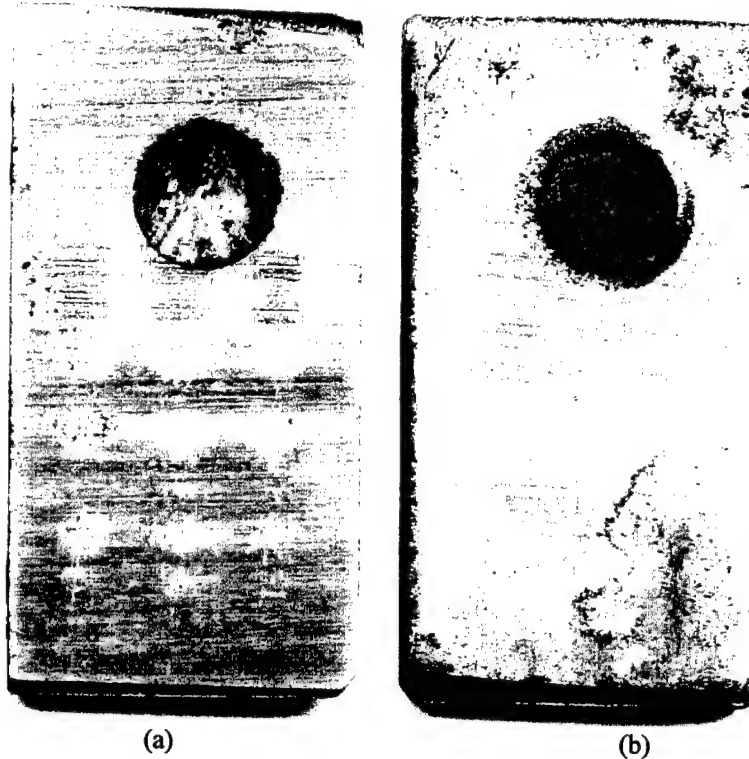


Figure 6. Corrosion products on AISI 4130 after 14 days galvanic cell test,
 (a) no. 4 exposed to 0.5N NaCl and (b) no. 2 exposed to 0.005N NaCl.

The resultant observations are that (1) the total oxide layer thickness for the sample exposed to the 0.5N NaCl solution was about twice that for the sample exposed to the 0.005N NaCl solution; (2) the sample exposed to the 0.5N NaCl solution had an outer layer of Fe_2O_3 (hematite) with a layer Fe_3O_4 (magnetite) adjacent to the steel with some residual NaCl in these oxides; (3) the sample exposed to the dilute 0.005N NaCl solution had thinner layers of both Fe_3O_4 and Fe_2O_3 compared to the thicker ones from the more concentrated 0.5N NaCl exposed sample; and (4) the relative volume fraction of the Fe_2O_3 phase in the total oxide coating was larger for the 0.5N NaCl exposed sample compared to that for the sample exposed to a lower concentration of NaCl.

Table 4. X-ray diffraction data for iron oxide phase analysis.

Raw X-ray Diffraction Data: for Corrosion Products Phase Analysis					
Most Intense Fe and Oxide Phase Lines (Fe substrate from Galvanic Cells)					
Phase	Bragg Angle	d-spacing	Primary Peak XRD Intensity (arb. Units) for:		
			Bare Fe	#2: 0.5N NaCl	#4: 0.005N NaCl
Fe (110)	44	2.0302	3800	1063	1332
Fe ₂ O ₃	37	2.4699		384	350
Fe ₃ O ₄	36	2.5311		640	692

Table 5. Interpretation of corrosion products from galvanic cell Fe substrates.

		Sample (bare or 0.xN NaCl exposed Fe)			Interpretation
line	Peak Intensity Ratios	Bare Fe	#2: 0.5N NaCl	#4: 0.005N NaCl	
a	Fe oxidized/Fe bare	1	0.28	0.35	#2 oxide layer twice as thick as #4
b	Fe ₂ O ₃ /Fe oxidized		0.6	0.52	#2 has more Fe ₂ O ₃ than #4
c	Fe ₂ O ₃ /Fe oxidized		0.36	0.26	#2 has more Fe ₂ O ₃ than #4
	ratio of c/b		0.6	0.5	Relative Ratio of Fe ₂ O ₃ /Fe ₃ O ₄ Phases is greater in #2 than #4

3.2 Engineering Evaluations

After exposure of “TACOM Joint A Assembly” samples to either SFT or CCT (for both phase I or II), the common interface was examined for corrosion products. An arbitrary, qualitative ranking methodology was devised to assign a metric for the extent of corrosion product formed at this interface and has been listed in Table 6. Observations of these common interfaces were qualitatively described and given a rating (where “zero” means no corrosion was observed, and “10” means the most extensive corrosion product buildup was observed) after either phase I or II exposures.

3.2.1 Salt Fog Exposure Results

Table 7 provides the interface corrosion assessment after salt fog exposure. Illustrative macrophotos of these interfaces after salt fog exposures are provided for the Ti-steel interfaces for phase I (Figure 7) and phase II (Figure 8).

3.2.2 Cyclic Corrosion Exposure Results

Figure 9 depicts the external macrostructure of all “TACOM Joint A Assembly” samples after phase II GM 9540P [3] accelerated testing exposure. Table 8 provides the interface corrosion assessment of these samples after phase I and II cyclic corrosion exposures. Illustrative

Table 6. "Joint A Assembly" interface corrosion rating system.

Rating	Qualitative Description	Reference
0(zero)	No Interface Corrosion	SF & GM phase I for Ti/Ti
1	No Significant Corrosion	SF phase I for Ti/Fe & Fe/Fe
2	Slight Corrosion (greater than for SF Ph I=#1)	GM phase I for Ti/Fe
3	Some Corrosion (greater than GM Ph I for Ti/Fe=#2)	GM phase I for Fe/Fe
4		
5	More Corrosion (greater than GM Ph I for Fe/Fe=#3)	SF phase II for Ti/Fe
6		
7	Severe Corrosion (greater than SF Ph II for Ti/Fe=#5)	SF phase II for Fe/Fe
8		
9	Very Severe Corrosion; Rust Exfoliation (less than for Fe/Fe=#10)	GM phase II for Ti/Fe
10	Most Severe Corrosion; Major Rust Exfoliation	GM Phase II for Fe/Fe

Table 7. "Joint A Assembly" interface corrosion assessment after salt fog exposure.

Couple	Rating	B117-90 Test Chamber Exposure, Phase I Qualitative Description	Rating	ASTM B117-90 Test Chamber Exposure, Phase II Qualitative Description
Ti/Ti	0	No Corrosion CARC Coating Sealed Out Moisture	0	No Ti Corrosion Moisture Intrusion into Common Interface
Ti/Fe	1	No Significant Corrosion of Fe CARC Coating Sealed Out Moisture	5	More Fe Corrosion (more than Ph I GM: Fe/Fe) Moisture Intrusion into Common Interface
Fe/Fe	1	No Significant Corrosion of Fe CARC Coating Sealed Out Moisture	7	Severe Fe Corrosion (more than Ph II SF: Ti/Fe) Moisture Intrusion into Common Interface

macrophotos of these interfaces after salt fog exposures are provided for the Ti-steel interfaces after phase I (Figure 10) and phase II (Figure 11). To be noted is that the buildup of interfacial corrosion products is even greater in the comparable Fe-Fe samples as listed in Tables 7 and 8 and illustrated in Figure 12 for salt fog and Figure 13 for cyclic corrosion phase II exposures. Clearly, the CCT protocol provides a more aggressive accelerated testing environment due to the programmed cyclic changes in thermal and chemical conditions compared to the constant exposure conditions within the SFT-accelerated testing chamber.

3.2.3 X-ray Characterization of Interface Corrosion Products From Post-Phase II (CCT and SFT) "TACOM Joint A Assembly" Samples

After phase II exposures, scrapings/flakes of the interfacial corrosion product were examined using the same x-ray diffraction techniques as were used for the previous scientific samples. The intent was to qualitatively determine if differences in the relative volume fractions of hematite and magnetite in the oxide occurred due to the two different accelerated testing methodologies.

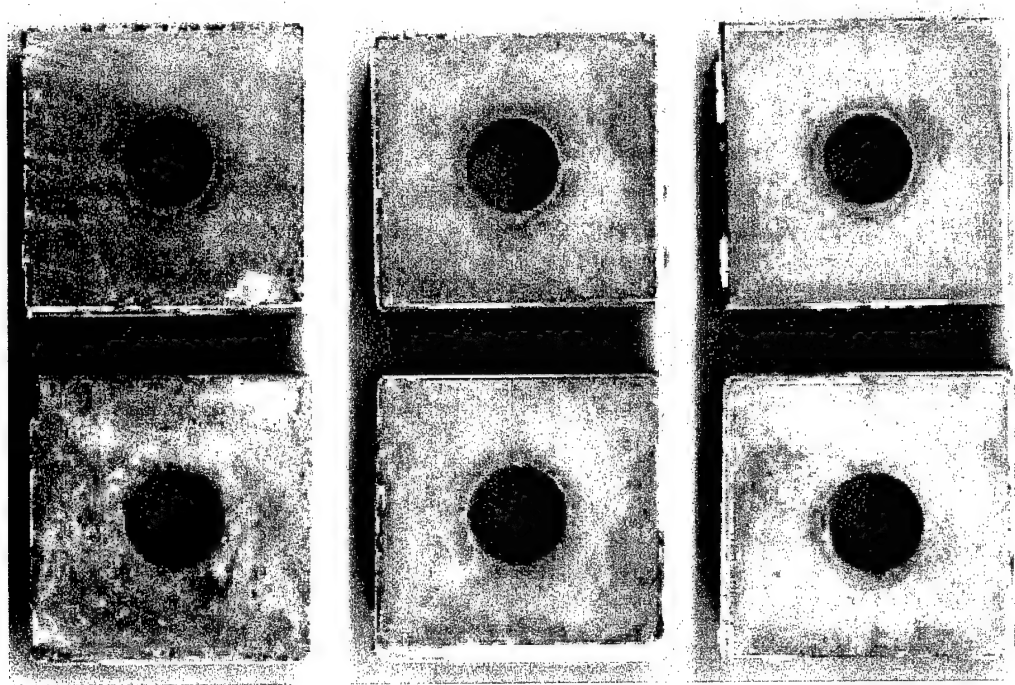


Figure 7. Macrophotos of Ti-steel interfaces after phase I salt fog exposure.

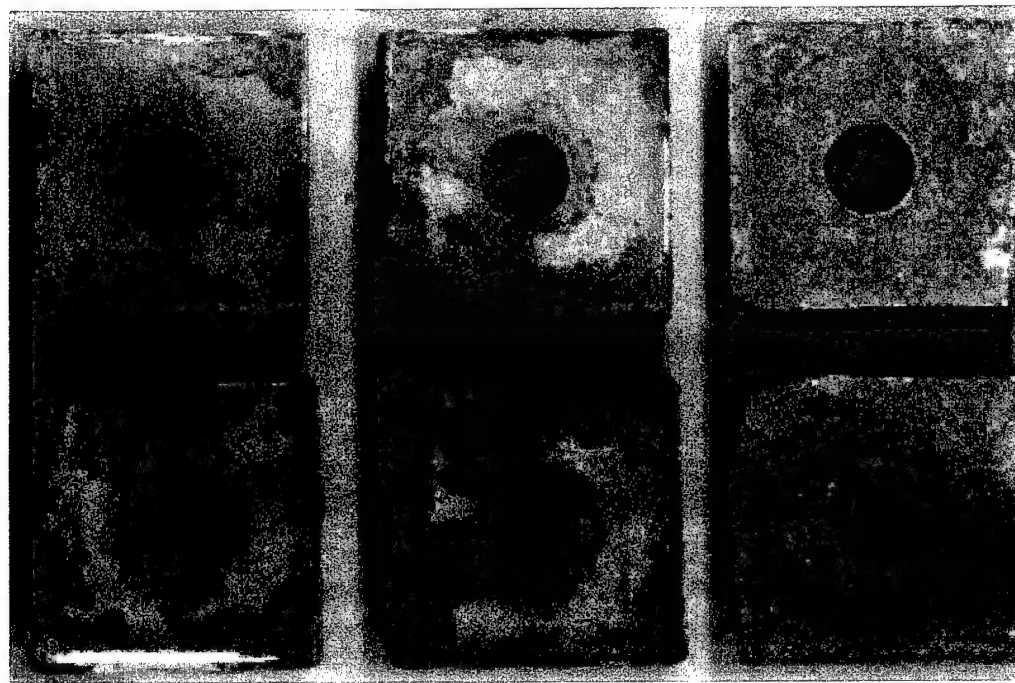


Figure 8. Macrophotos of Ti-steel interfaces after phase II salt fog exposure.

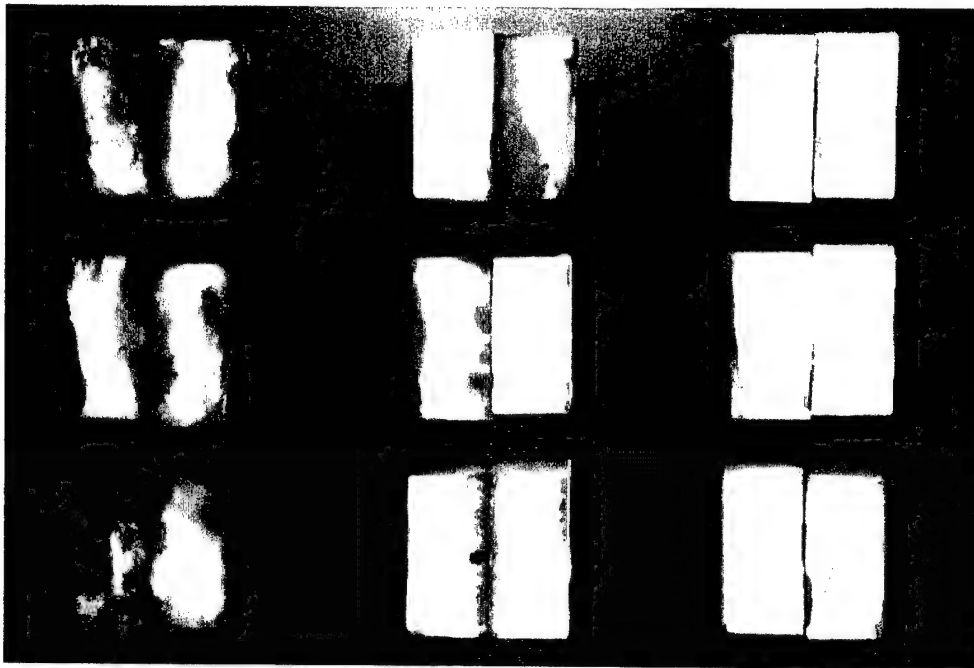


Figure 9. Assembled armor mockup couples after phase II GM 9540P testing exposure.

Table 8. "Joint A Assembly" interface corrosion assessment after cyclic corrosion exposure.

Couple	Rating	Cyclic Corrosion Test Chamber Exposure, Phase I Qualitative Description	Rating	Cyclic Corrosion Test Chamber Exposure, Phase II Qualitative Description
Ti/Ti	0	No Corrosion Thermal Cycles Slightly Compromised CARC Seal --leading to slight moisture intrusion	0	No Ti Corrosion Moisture Intrusion into Common Interface
Ti/Fe	2	Slight Corrosion of Fe (more than Ph I SF:Ti/Fe) Thermal Cycles Slightly Compromised CARC Seal --leading to slight moisture intrusion	9	Very Severe Fe Corrosion (more than Ph II SF:Fe/Fe) --Rust Exfoliation Moisture Intrusion into Common Interface
Fe/Fe	3	Some Fe Corrosion (more than Ph I SF:Fe/Fe) Thermal Cycles Slightly Compromised CARC Seal --leading to slight moisture intrusion	10	Most Severe Fe Corrosion; Major Rust Exfoliation Moisture Intrusion into Common Interface

The results listed in Table 9 indicate that at Fe/Fe interfaces the salt fog exposures produced a primarily hematite oxide phase while the cyclic corrosion produced a primarily magnetite product. For samples with Ti/Fe interfaces, the volume fraction of the minority oxide seems to be increased for either testing protocol.

4. Conclusions

4.1 Scientific Studies

An initial Ti (6/4)-Fe (AISI 4130) galvanic corrosion database for an aqueous environment was established. Potentiodynamic scans using a conventionally accepted open cell with a 3.5% NaCl aqueous solution validated that a more noble Ti cathode increased the mixed couple galvanic current by an order of magnitude, thus increasing the corrosion rate at the (4130) steel anode.

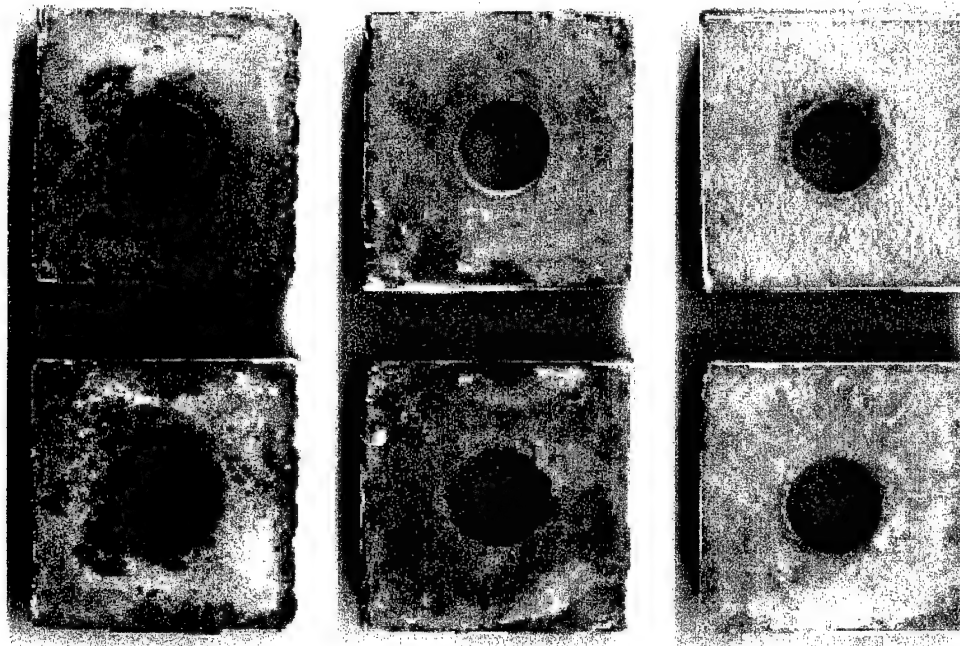


Figure 10. Macrophotos of Ti-steel interfaces after phase I cyclic corrosion exposure.

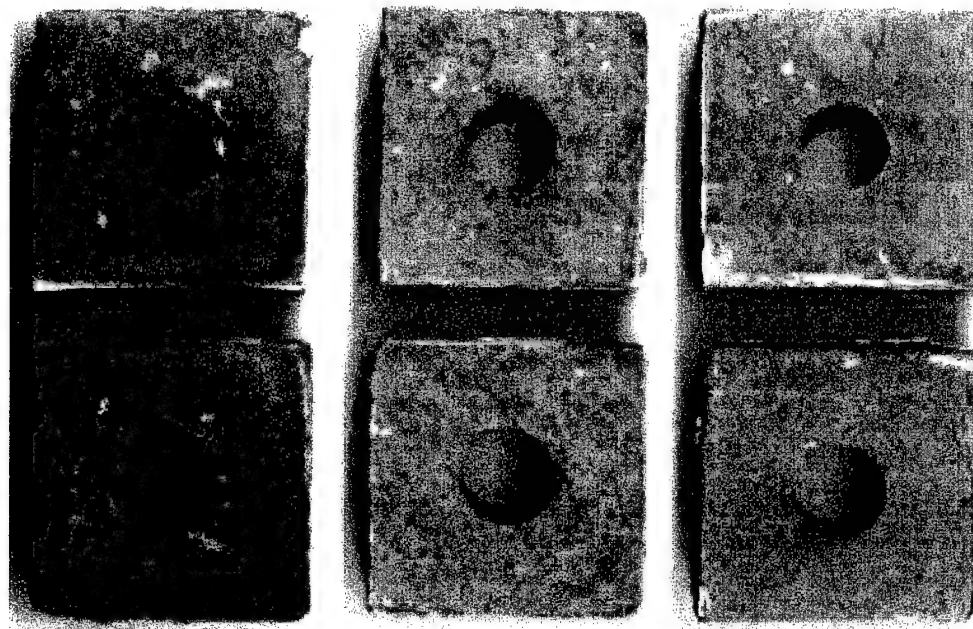


Figure 11. Macrophotos of Ti-steel interfaces after phase II cyclic corrosion exposure.

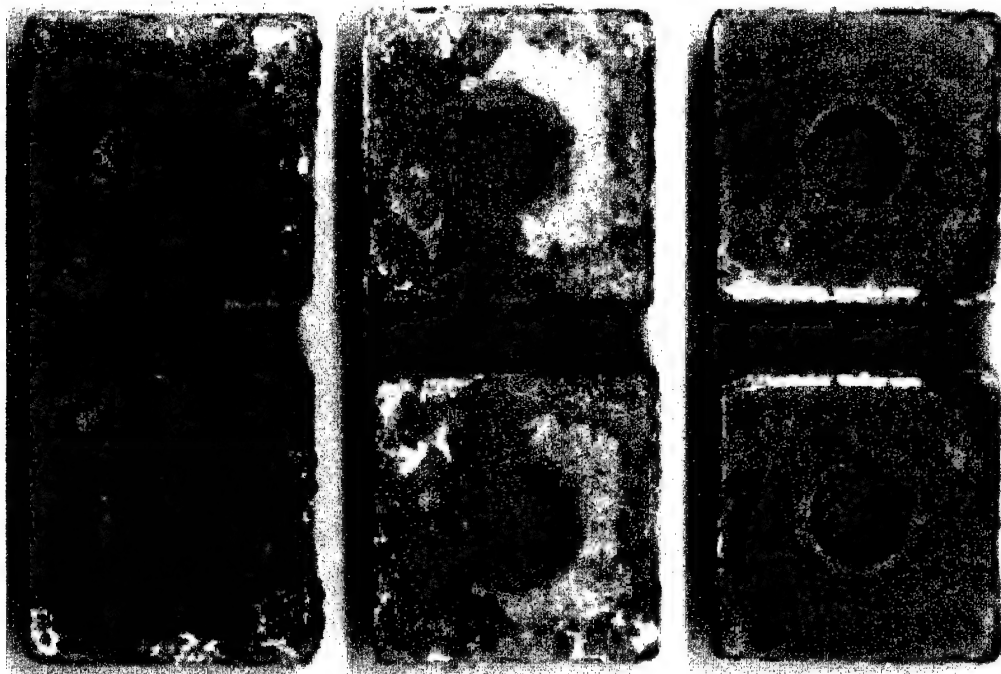


Figure 12. Macrophotos of Fe-Fe interfaces after phase II salt fog exposure.

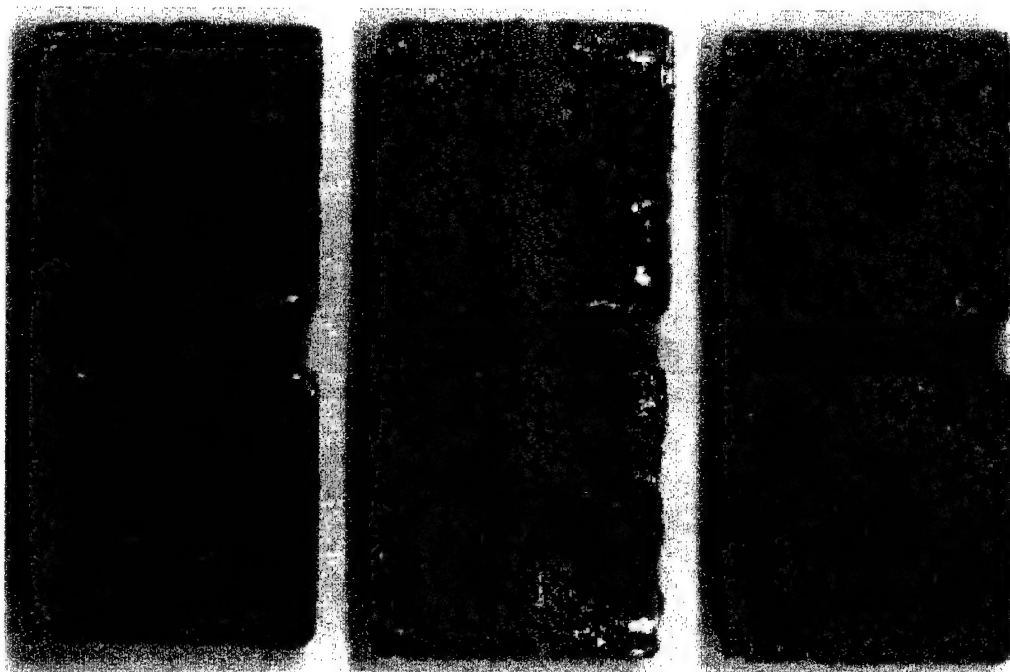


Figure 13. Macrophotos of Fe-Fe interfaces after phase II cyclic corrosion exposure.

Table 9. Interface oxidation products for “Joint A Assembly” samples from x-ray diffraction analysis.

Sample Descriptors		Estimated Amounts of Interface Corrosion Product(s) after Phase II		
ID	Couple	Comments	After Salt Fog Exposure	After GM 9540 Exposure
A	Fe/Fe		Fe_2O_3 Primary Phase; Fe_3O_4 minor	
B	Fe/Fe			Fe_3O_4 Primary Phase; Fe_2O_3 minor
E	Ti/Fe	Ti & Fe side scrapings	Mix of Fe_3O_4 (55%) & Fe_2O_3	
V	Ti/Fe	Fe side scraping only	Nearly equal mix of Fe_3O_4 & Fe_2O_3	
R	Ti/Fe	Scrapings only from Ti side		Mix of Fe_3O_4 (60%) & Fe_2O_3 (40%)
X	Ti/Fe	Flakes only from Fe side		Major Fe_3O_4 Phase; very minor Fe_2O_3
Y	Ti/Fe	Fine powder only from Fe side		Major Fe_3O_4 Phase; very minor Fe_2O_3

During galvanic cell testing of the bare Ti/Fe couples, the buildup of an oxide layer on the Fe anode was faster and thicker in the 0.5N NaCl than in the 0.005N NaCl electrolyte cell. The presence of this oxide layer effectively increased the electrical resistance of this circuit for either concentration electrolyte cell nominally reducing the steady state galvanic current to half of the initial maximum current observed. In both cases, magnetite was the major oxide phase formed but the minority volume fraction was higher for the hematite phase formed in the 0.5N NaCl cell; this shift may be a result of the differences in the kinetics of oxide formation.

No galvanic current was measured during galvanic cell testing of the CARC coated Ti/Fe couples for either NaCl concentration cell; thus the CARC layer was very protective in isolating both the anode and cathode from the electrolyte. For both NaCl concentration cells, even deliberate X-scribed defects in the CARC experienced rapid buildup of a corrosion product in the defect. Thus, compared to the bare couples, the measured galvanic current was reduced by two orders of magnitude for the 0.005N NaCl cell and three orders of magnitude for the 0.5N NaCl cell, respectively. This means that as a practical matter, small defects in CARC should experience a rapid buildup of an oxide product that could partially block subsequent electrolyte access to the rest of the steel substrate.

4.2 Engineering Studies

Accelerated “TACOM Joint A Assembly” SFT of phase I samples that had unbroken CARC seals between the Ti/Fe plates had virtually no corrosion along the contacting iron interface because there was no fluid intrusion. Similar accelerated “TACOM Joint A Assembly” cyclic corrosion testing of phase I samples had minor corrosion along the contacting iron interface due to localized compromises in the CARC seal between the Ti/Fe plates. Thus, in most cases, the presence of a quality CARC coating can help exclude electrolytes between contacting dissimilar metal plates, thus mitigating galvanically induced corrosion product buildup.

During phase II accelerated “TACOM Joint A Assembly” salt fog and cyclic corrosion testing, the absence of the CARC seal allowed the intrusion of moisture/electrolyte into the crevasse between the two bolted plates leading to corrosion at the contacting iron interface. Thus, there was a significant buildup of Fe corrosion products in the crevasse between both Fe/Fe and Ti/Fe interfaces during salt fog exposures. For Fe/Fe couples, hematite was the primary oxide phase with a minor amount of magnetite; for Ti/Fe couples, the presence of Ti apparently produced a

nearly even mix of both magnetite and hematite but the total quantity of corrosion product was less than for the Fe/Fe couples.

For cyclic corrosion phase II exposures there was severe oxidation/exfoliation of corrosion products again due to the presence of moisture/electrolyte in the crevasse between either the Fe/Fe or Ti/Fe interfaces. For Fe/Fe couples, magnetite was the primary oxide phase with a minor amount of hematite; for Ti/Fe couples the presence of Ti 6/4 apparently caused the formation of an oxide mixture of mainly magnetite with some hematite, but the quantity of corrosion product was again less than for the Fe/Fe couples.

To be noted is that phase II CCT Fe/Fe samples produced the greatest amount of interfacial corrosion products for all samples examined in this study. Thus, clearly for an engineering corrosion propensity screening tool, the CCT protocol—due to the programmed cyclic changes in thermal and chemical conditions compared to the constant exposure conditions within the SFT-accelerated testing chamber—provides a more rigorous and aggressive accelerated testing methodology.

Thus, mixed Ti/Fe interfaces that are protected/sealed from the environment by CARC coatings will not experience unacceptable galvanically accelerated corrosion phenomena. Accordingly, mixing titanium and steel components on U.S. Army materiel, provided they are protected by a quality CARC coating, will not cause adverse durability problems or lead to increased maintenance issues and costs.

5. References

1. Montgomery, J. S., M. G. H. Wells, B. Roopchand, and J. S. Ogilvy. "Low-Cost Titanium Armors for Combat Vehicles." *Journal of Metals*, vol. 49, no. 5, pp. 45–47, May 1997.
2. American Society for Testing and Materials. "Standard Method of Salt Spray (Fog) Testing." ASTM B117, West Conshohocken, PA, 1990.
3. General Motors. "Accelerated Corrosion Test GM 9540P." General Motors Engineering Standard GM 9540P, 1997.
4. Levy, M., B. E. Placzankis, R. Brown, R. Huie, M. Kane, and G. McAllister. "The Effects of Co-Mingling Dissimilar Fastener Coatings on the Corrosion Behavior of Steel Bolt Assemblies." MTL TR 92-40, U.S. Army Materials Technology Laboratory, Watertown, MA, July 1992.
5. U.S. Department of Defense. "Primer (Wash) Pretreatment (Formula No. 117 for Metals)." DOD-P-15328, revision D, amendment 2, Washington, DC, March 1991.
6. U.S. Department of Defense. "Primer, Epoxy Coating, Corrosion Inhibiting, Lead and Chromate Free." MIL-P-53022-10, Washington, DC, February 1992.
7. U.S. Department of Defense. "Coating. Aliphatic Polyurethane, Single Component, Chemical Agent Resistant." MIL-C-53039A, Washington, DC, May 1993.
8. Miller, C. E., J. H. Beatty, J. V. Kelley, B. E. Placzankis, and P. F. Buckley. "Galvanic and Potentiodynamic Corrosion Studies of Depleted Uranium and Sabot Materials." ARL-TR-2047, U.S. Army Research Laboratory, Aberdeen Proving Ground, MD, September 1999.
9. Cullity, B. D. *Elements of X-ray Diffraction*. Second Edition, Reading, MA: Addison-Wesley, chapters 6, 7, and 10.

INTENTIONALLY LEFT BLANK.

REPORT DOCUMENTATION PAGE			Form Approved OMB No. 0704-0188
<p>Public reporting burden for this collection of information is estimated to average 1 hour per response, including the time for reviewing instructions, searching existing data sources, gathering and maintaining the data needed, and completing and reviewing the collection of information. Send comments regarding this burden estimate or any other aspect of this collection of information, including suggestions for reducing this burden, to Washington Headquarters Services, Directorate for Information Operations and Reports, 1215 Jefferson Davis Highway, Suite 1204, Arlington, VA 22202-4302, and to the Office of Management and Budget, Paperwork Reduction Project (0704-0188), Washington, DC 20503.</p>			
1. AGENCY USE ONLY (Leave blank)	2. REPORT DATE	3. REPORT TYPE AND DATES COVERED	
	September 2002	Final, January 2000-December 2001	
4. TITLE AND SUBTITLE	Galvanic Behavior Database for Titanium-Steel Alloy Couples		5. FUNDING NUMBERS
6. AUTHOR(S)	Ralph P. I. Adler, Christopher E. Miller, and Brian E. Placzankis		VEPRO 3H
7. PERFORMING ORGANIZATION NAME(S) AND ADDRESS(ES)	U.S. Army Research Laboratory ATTN: AMSRL-WM-MC Aberdeen Proving Ground, MD 21005-5069		8. PERFORMING ORGANIZATION REPORT NUMBER
9. SPONSORING/MONITORING AGENCY NAMES(S) AND ADDRESS(ES)			10. SPONSORING/MONITORING AGENCY REPORT NUMBER
11. SUPPLEMENTARY NOTES			
12a. DISTRIBUTION/AVAILABILITY STATEMENT	Approved for public release; distribution is unlimited.		12b. DISTRIBUTION CODE
<p>13. ABSTRACT (Maximum 200 words)</p> <p>Future lightweight armor for the next generation of lighter material will probably use titanium alloy components. These will form galvanic couples with other materials and may induce phenomena accelerating the corrosion rate of those metals less noble than titanium. The project objective was to evaluate the magnitude of galvanic corrosion between typical ferrous and titanium alloys. Electrochemical and accelerated corrosion measurements on both bare and Chemical agent resistant coatings (CARC)-coated Ti/steel samples determined accelerated corrosion rates. Samples with and without "X-scribed" defects in the CARC coating were evaluated. Electrochemical studies on bare Ti/steel couples validated accelerated steel corrosion rates but found that intact CARC coatings mitigate corrosion. Even for X-scribed samples, the rapid corrosion product buildup in the defect reduced galvanic currents by two orders of magnitude. Studies with "Joint A Assembly" CARC-coated samples (phase I: bolted sets of Ti/steel plates with intact CARC seals) had virtually no interface corrosion. After examination, the rebolted samples with compromised CARC seals had a second accelerated corrosion cycle (phase II); the moisture intrusion caused a severe buildup of interface corrosion. Thus Ti/Fe interfaces with defect-free CARC coatings can prevent buildup of iron corrosion products.</p>			
14. SUBJECT TERMS	corrosion, titanium, steel, CARC coating		15. NUMBER OF PAGES
			25
16. PRICE CODE			
17. SECURITY CLASSIFICATION OF REPORT	18. SECURITY CLASSIFICATION OF THIS PAGE	19. SECURITY CLASSIFICATION OF ABSTRACT	20. LIMITATION OF ABSTRACT
UNCLASSIFIED	UNCLASSIFIED	UNCLASSIFIED	UL

INTENTIONALLY LEFT BLANK.